

Assessment of Power System Stability by UPFC with Two Shunt Voltage-Source Converters and a Series Capacitor

Farzad Mohammadzadeh Shahr¹, Ebrahim Babaei^{*2}

Faculty of Electrical and Computer Engineering, University of Tabriz, Tabriz, Iran

¹f-mohammadzadeh@iau-ahar.ac.ir; ^{*2}e-babaei@tabrizu.ac.ir

Abstract

In this paper, the effects of a newly presented structure of unified power flow controller (UPFC) which is based on two shunt voltage-source converters and a series capacitor, are investigated on the dynamic stability of power system. A power system including the newly presented structure of UPFC is introduced to examine this. The non-linear dynamic model of the system under investigation and its non-linear equations are presented as well. The linear equations are achieved by linearizing the non-linear equations around the operation point. A modified Heffron-Philips model is proposed through the linearized equations of the investigated system. The state equations of the system are then extracted using the modified Heffron-Philips model. The damping controller of UPFC is then presented and its control parameters are calculated by phase compensation method. Finally, the most effective input signal of UPFC control signals is selected using some techniques. The validity of the theoretical investigations is confirmed by simulation results obtained in MATLAB/Simulink.

Keywords

UPFC Modeling; FACTS Device; Electromechanical Oscillations Damping; Low Frequency Oscillations; Modified Heffron-Philips Model

Nomenclature

M	Inertia constant (second)
$X_{E,g}$ for $g = 1, 2$	Transformer g reactance (pu)
$X_{se,k}$ for $k = a, b, c$	Equivalent reactance of capacitor in k phase (pu)
X_i for $i = d, q$	Steady state synchronous reactance of the generator on i axis (pu)
X'_d	Direct axis transient synchronous reactance of the generator (pu)
X_{bv}	Reactance of transmission line (pu)
X_{sc}	Reactance of transformer (pu)
C_{dc}	Dc link capacitor (pu)
C_{sc}	Series capacitor (pu)
$R_{E,g}$ for $g = 1, 2$	Equivalent resistance of shunt converter g (pu)
I_b for $i = d, q$	Current in infinite bus on i axis (pu)

$I_{i,i}$ for $i = d, q$	Current of phase k in transmission line on i axis (pu)
$I_{se,i}$ for $i = d, q$	Current of phase k in series capacitor on i axis (pu)
$I_{E,g,i}$ for $g = 1, 2$ $i = d, q$	Current in converter g on i axis (pu)
V_{dc}	Voltage at dc link (pu)
$V_{se,k}$ for $k = a, b, c$	Series capacitor voltage of k phase (pu)
V_b	Voltage at infinite bus (pu)
V_i	Voltage at generator terminal (pu)
$V_{t,i}$ for $i = d, q$	Terminal voltage on i axis (pu)
V_{ref}	Reference voltage (pu)
ΔT_{UPFC}	Provided electrical torque by UPFC damping controller (pu)
P_m	Input mechanical power to the generator (pu)
P_e	Electrical power of the generator (pu)
A	State matrix
B	Input matrix
C	Output matrix
D	Direct transfer matrix
X	State vector
Y	Output vector
U	Input vector
$F(s)$	Forward path of the UPFC damping controller
$K_c(s), K_o(s), K_L(s), K_M(s)$	UPFC damping controller transformer controls
$H(s)$	Transfer function of UPFC damping controller
f_s	Switching frequency (Hz)
δ	Phase angle of System load (degree)
$\Delta\delta$	Phase angle deviation of System load (degree)
$\delta_{E,g}$ for $g = 1, 2$	Phase angle of shunt converter g (degree)
$\Delta\delta_{E,g}$ for $g = 1, 2$	Phase angle deviation of shunt voltage source converter g (degree)
$m_{E,g}$ for $g = 1, 2$	Pulse width modulation index of shunt converter g
$\Delta m_{E,g}$ for $g = 1, 2$	Pulse width modulation index deviation of shunt voltage source converter g
ω_0	Fundamental angle frequency ($rad\ s^{-1}$)
ω_i	Oscillation angle frequency ($rad\ s^{-1}$)
$\Delta\omega$	Error signal ($rad\ s^{-1}$)
D_m	Friction factor of generator

D_{UPFC}	Friction factor of the UPFC damping controller
u_k	Input signal of the UPFC
$\Psi(\mu)$	System operation domain
K_U	UPFC controller gain
K_a	Gain of AVR in generator
$K_1 - K_{12}$	Constants of Heffron-Phillips model
$K_{c,ak}, K_{p,ak}, K_{q,ak}, K_{r,ak}, K_{se,ak}$	Constants control of input signals
K_{qd}, K_{pd}, K_{vd}	Constant control of input signal
T'_{do}	Direct axis open circuit time constant of the generator (second)
T_a	Time constant of the generator of AVR
$T_1, T_2, T_3, T_4, T_U, T_W$	Time constants of phase compensator

Introduction

Nowadays, considering the increasing growth of power systems in different countries and their mutual connections and also the great interest in transmitting the possible maximum power through the transmission lines, the maintenance and enhancement of power systems stability becomes more important [Shahir (2013), Kundor (1994)]. The modern power systems are designed to achieve high generation capacities, bringing more risk into power systems stability. One of the most important factors threatening power systems stability is the electromechanical oscillation of the generator. Dynamic instability is raised due to balance lose between the output electric power and input mechanical power, lack of damping torque, and sudden load distortion outbreak. The frequency of such oscillations falls in the range of one to few Hertz [Shahir (2013)]. Several factors such as operation condition, load characteristics, lines impedance and power, series capacitors, and voltage regulators influence this type of oscillations.

One of the most effective solutions is to install power system stabilizer (PSS) in generator location to damp the electromechanical oscillations [Yassami (2010)]. The PSS generates a complementary signal to rapidly damp the distortions caused by oscillations of power system. The PSS usually considers frequency error signal as its input and generates a signal added to the voltage. The practical and simulation results show that the PSS will be highly effective in system oscillations damping if it is properly regulated.

Recent technology development in semiconductor based devices and their control techniques field and high interest of power systems designers in utilizing flexible ac transmission systems (FACTS) for maximum power transmission has provided a new stability

research field. The application of Applying FACTS devices brings about more reliability and less costs in different network arrangements under distortions occurrence conditions [Song (2004), Xia (2010)]. Among the FACTS devices, the voltage-source based converters considerably affect the transient state and improve dynamic stability of power systems [Hingorani (1999)]. The UPFC, one of the most important and effective FACTS device applied in series-shunt mode consists of a series and a shunt three-phase two-level converter connected to each other through a dc capacitor. The series converter controls the active and reactive powers of transmission line by controlling the amplitude and phase angle of series voltage and the shunt converter compensates the UPFC losses and stabilizes dc link voltage in addition to transmission line reactive power control [Sarvana (2009)]. Many different structure have been proposed for UPFC [Shahir (2012), Sadigh (2010)]. In [Sadigh (2010)], a new UPFC structure consisting of two shunt voltage-source converters and a dc capacitor installed between the mentioned converters is presented in which the UPFC parameters are controlled by the series capacitor. The voltage and the current of the series capacitor are controlled by the operation of the two shunt converters [Sadigh (2010)]. The control and the measuring systems of conventional UPFCs are separately designed due to the different insulation and protection processes of series and shunt converters. This leads to high time and cost expenditure of such devices design and manufacturing. In the structure of UPFC presented in [Sadigh (2010)], the evaluation bulk is decreased due to similar shunt converters application and as a result; the control and measuring systems design and manufacturing costs are significantly decreased. Also, in comparison with congenital UPFC, total VA rating for high active and reactive power flow control is decreased. In the structure of [Sadigh (2010)], the signals could be applied as UPFC input signals for stability and electromechanical oscillations control that is an advantage of that structure. Three signals can be applied for stability control in conventional UPFCs [Shahir (2012)], while four signals are used to control the operation of the newly presented UPFC. Reduction of the THD value of the injected series voltage and applying series capacitor as constant series capacitive compensator during converter 2 standby interval are other advantages of the structure presented in [Sadigh (2010)].

The modeling process of conventional UPFCs and its effect on dynamic stability is investigated in [Fang (2003)] and transient stability rate improvement is evaluated in [Sreenivasachar (2000)]. In this paper, the

effects of the UPFC structure presented in [Sadigh (2010)] on the dynamic stability and electromechanical oscillations damping of power system are investigated. The analysis starts by nonlinear equations extraction. The linear equations and the modified Heffron-Philips model are obtained by linearizing the nonlinear equations around the system operation point. The phase compensator technique [Larsen (1995), Chandrakar (2010)] is then applied and the proper controller is designed and regulated. Finally, the most effective input signal for UPFC control is obtained by simulating the system in MATLAB/Simulink to damp the oscillations of synchronous generator's rotor.

Investigated System

A sample power system including a single machine with infinite bus along with the UPFC presented in [Sadigh (2010)] is used to investigate the dynamic stability. The single line structure of the investigated power system is illustrated in Fig. 1. The utilized UPFC consists of two parallel transformers, a series capacitor and two shunt voltage-source converters controlled by pulse width modulation (PWM) technique [Shahir (2012)]. Here, $R_{E,1}$ and $R_{E,2}$ are neglected in comparison with $X_{E,1}$ and $X_{E,2}$, respectively.

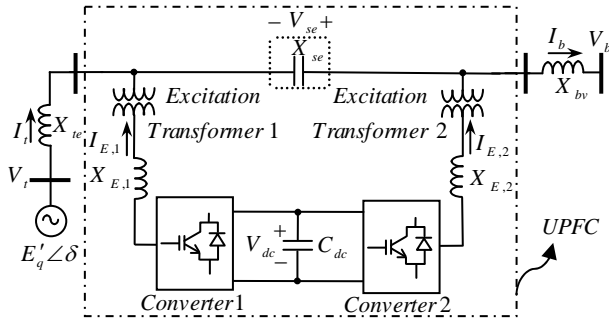


FIG. 1 THE SINGLE LINE DIAGRAM OF INVESTIGATED SYSTEM

Dynamic Modeling of the Investigated Power System

Nonlinear Dynamic Model

All reactance and resistances of the generator, transformers, and transmission line should be considered for nonlinear dynamic modeling of power system. Therefore, the following nonlinear equations are obtained assessing the system shown in Fig. 1:

$$\dot{\delta} = \omega_0(\omega - 1) \quad (1)$$

$$\dot{\omega} = \frac{P_m - P_e - D_m \Delta \omega}{M} \quad (2)$$

$$\dot{E}'_q = \frac{-E_q + E_{fd}}{T'_{do}} \quad (3)$$

$$\dot{E}_{fd} = \frac{-E_{fd} + K_a (V_{ref} - V_t)}{T_a} \quad (4)$$

$$\begin{aligned} \dot{V}_{dc} = & \frac{3m_{E,1}}{4C_{dc}} \begin{bmatrix} \cos \delta_{E,1} & \sin \delta_{E,1} \end{bmatrix} \begin{bmatrix} I_{E,1,d} \\ I_{E,1,q} \end{bmatrix} \\ & + \frac{3m_{E,2}}{4C_{dc}} \begin{bmatrix} \cos \delta_{E,2} & \sin \delta_{E,2} \end{bmatrix} \begin{bmatrix} I_{E,2,d} \\ I_{E,2,q} \end{bmatrix} \end{aligned} \quad (5)$$

$$\dot{V}_{se} = \frac{1}{C_{se}} I_{se,i} \quad \text{for } i = d, q \quad (6)$$

The followings are valid for (1)-(6):

$$P_e = V_{t,d} I_{t,d} + V_{t,q} I_{t,q}; E_q = E'_q + (X_d - X'_d) I_{t,d};$$

$$V_t = V_{t,d} + jV_{t,q}; V_{t,d} = X_q I_{t,q}; V_{t,q} = E'_q - X'_d I_{t,d};$$

$$I_{t,d} = I_{se,d} + I_{E,1,d}; I_{t,q} = I_{se,q} + I_{E,1,q};$$

$$I_{se,d} = a_1 V_b \cos \delta + \frac{b_1 m_{E,2} V_{dc}}{2} \cos \delta_{E,2} + c_1 E'_q + \frac{d_1 m_{E,1} V_{dc}}{2} \cos \delta_{E,1}$$

$$I_{se,q} = a_1 V_b \sin \delta + \frac{b_1 m_{E,2} V_{dc}}{2} \sin \delta_{E,2} + \frac{d_1 m_{E,1} V_{dc}}{2} \sin \delta_{E,1}$$

$$I_{E,1,d} = a_2 V_b \cos \delta + \frac{b_2 m_{E,2} V_{dc}}{2} \cos \delta_{E,2} + c_2 E'_q + \frac{d_2 m_{E,1} V_{dc}}{2} \cos \delta_{E,1}$$

$$I_{E,1,q} = a_2 V_b \sin \delta + \frac{b_2 m_{E,2} V_{dc}}{2} \sin \delta_{E,2} + \frac{d_2 m_{E,1} V_{dc}}{2} \sin \delta_{E,1}$$

$$I_{E,2,d} = a_3 V_b \sin \delta + \frac{b_3 m_{E,2} V_{dc}}{2} \cos \delta_{E,2} + c_3 E'_q + \frac{d_3 m_{E,1} V_{dc}}{2} \cos \delta_{E,1}$$

$$I_{E,2,q} = a_3 V_b \sin \delta + \frac{b_3 m_{E,2} V_{dc}}{2} \sin \delta_{E,2} + \frac{d_3 m_{E,1} V_{dc}}{2} \sin \delta_{E,1}$$

$$I_{t,d} = (a_1 + a_2)V_b \cos \delta + (b_1 + b_2) \frac{m_{E,2} V_{dc}}{2} \cos \delta_{E,2}$$

$$+(c_1+c_2)E'_q+(d_1+d_2)\frac{m_{E,1}V_{dc}}{\gamma}\cos\delta_{E,1}$$

$$I_{t,q} = (a_1 + a_2)V_b \sin \delta + (b_1 + b_2) \frac{m_{E,2} V_{dc}}{\gamma} \sin \delta_{E,2}$$

$$+ (d_1 + d_2) \frac{m_{E,1} V_{dc}}{2} \sin \delta_{E,1}$$

$$X_{BB} = X_{E,2} + X_{bv}; X_{a1} = X_{se} + X_{E,1}X_{te} + X_{te}X_{se};$$

$$X_{a2} = X_{BB}X_{E,1}; X_{a3} = X_{E,2}X_{E,1}; X_{b1} = X_{E,1} + X_{te};$$

$$X_{b1} = X_{E,1} + X_{te}; X_{b2} = X_{E,2} X_{bv}; X_{b3} = X_{BB} X_{se};$$

$$X_1 = X_{a1}X_{a2} + X_{b1}X_{b2}; X_2 = X_{bv} + \frac{X_{bv}X_{te}}{X_{E1}};$$

The other constants are presented in Appendix A.

Linear Dynamic Model

The linear dynamic model of the sample system is obtained linearizing (1)-(6) around the system operation point. The following equations are obtained after linearization:

$$\Delta \dot{\delta} = \omega_0 \Delta \omega \quad (7)$$

$$\Delta \dot{\omega} = \frac{\Delta P_m - \Delta P_e - D \Delta \omega}{M} \quad (8)$$

$$\Delta \dot{E}'_q = \frac{-\Delta E_q + \Delta E_{fd}}{T'_{do}} \quad (9)$$

$$\Delta \dot{E}_{fd} = \frac{-\Delta E_{fd} + K_a (\Delta V_{ref} - \Delta V_t)}{T_a} \quad (10)$$

$$\Delta \dot{V}_{dc} = K_7 \Delta \delta + K_8 \Delta E'_q - K_9 \Delta V_{dc} + K_{c,E,1} \Delta m_{E,1} + K_{c,\delta E,1} \Delta \delta_{E,1} + K_{c,E,2} \Delta m_{E,2} + K_{c,\delta E,2} \Delta \delta_{E,2} \quad (11)$$

$$\Delta \dot{V}_{se} = K_{10} \Delta \delta + K_{11} \Delta E'_q + K_{s1} \Delta m_{E,2} + K_{s2} \Delta m_{E,1} + K_{12} \Delta V_{dc} + K_{s3} \Delta \delta_{E,2} + K_{s4} \Delta \delta_{E,1} \quad (12)$$

The followings are valid in (7)-(12):

$$\Delta P_e = K_1 \Delta \delta + K_2 \Delta E'_q + K_{p,E,1} \Delta m_{E,1} + K_{p,\delta E,1} \Delta \delta_{E,1} + K_{p,E,2} \Delta m_{E,2} + K_{p,\delta E,2} \Delta \delta_{E,2} + K_{pd} \Delta V_{dc} \quad (13)$$

$$\Delta E_q = K_4 \Delta \delta + K_3 \Delta E'_q + K_{q,E,1} \Delta m_{E,1} + K_{q,\delta E,1} \Delta \delta_{E,1} + K_{q,E,2} \Delta m_{E,2} + K_{q,\delta E,2} \Delta \delta_{E,2} + K_{qd} \Delta V_{dc} \quad (14)$$

$$\Delta V_t = K_5 \Delta \delta + K_6 \Delta E'_q + K_{v,E,1} \Delta m_{E,1} + K_{v,\delta E,1} \Delta \delta_{E,1} + K_{v,E,2} \Delta m_{E,2} + K_{v,\delta E,2} \Delta \delta_{E,2} + K_{vd} \Delta V_{dc} \quad (15)$$

The constants used in (11)-(15) are presented in details in Appendix B.

The Proposed Modified Heffron-Philips Model

Here, it is possible to propose the modified Heffron-Philips model of the system shown in Fig. 1 based on (7)-(12) to analyse and investigate the system stability against oscillations and to evaluate its small-signal stability [Shahir (2012), Kundor (1994)]. The proposed modified Heffron-Philips model is a linear model applied in low frequency oscillations and small signal stability investigations. Fig. 2 shows the block diagram of the proposed modified Heffron-Philips model resulted from (7)-(12). In this model, one of the linearized control signals of the sample power system including UPFC, $\Delta m_{E,1}$, $\Delta m_{E,2}$, $\Delta \delta_{E,1}$, and $\Delta \delta_{E,2}$ is applied to the UPFC and controls the investigated UPFC's operation.

The block diagram of proposed modified Heffron-Philips model shown in Fig. 2 contains 35 constants that can be defined as row vectors of $K_{p,uk}$, $K_{q,uk}$, $K_{v,uk}$, $K_{c,uk}$, and $K_{se,uk}$ as follows to simplify the calculations:

$$K_{p,uk} = [K_{p,E,1} \quad K_{p,\delta E,1} \quad K_{p,E,2} \quad K_{p,\delta E,2}] \quad (16)$$

$$K_{q,uk} = [K_{q,E,1} \quad K_{q,\delta E,1} \quad K_{q,E,2} \quad K_{q,\delta E,2}] \quad (17)$$

$$K_{v,uk} = [K_{v,E,1} \quad K_{v,\delta E,1} \quad K_{v,E,2} \quad K_{v,\delta E,2}] \quad (18)$$

$$K_{c,uk} = [K_{c,E,1} \quad K_{c,\delta E,1} \quad K_{c,E,2} \quad K_{c,\delta E,2}] \quad (19)$$

$$K_{se,uk} = [K_{s,E,1} \quad K_{s,\delta E,1} \quad K_{s,E,2} \quad K_{s,\delta E,2}] \quad (20)$$

The row vectors of (16)-(20), are applied on proposed modified Heffron-Philips system as the following input vector:

$$U = [\Delta m_{E,1} \quad \Delta \delta_{E,1} \quad \Delta m_{E,2} \quad \Delta \delta_{E,2}]^T \quad (21)$$

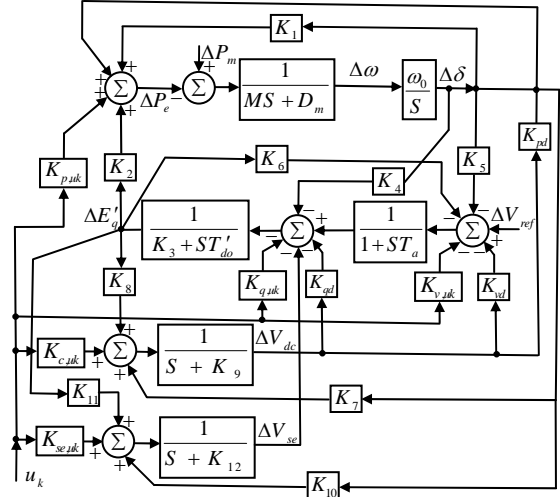


FIG. 2 THE PROPOSED MODIFIED HEFFRON-PHILIPS MODEL OF INVESTIGATED SYSTEM

The State Equations of the Investigated System

Based on (7)-(15), the dynamic model of the investigated system in the form of the state space equation can be expressed as follows:

$$\dot{X} = AX + BU \quad (22)$$

where X and U are defined as follows:

$$X = [\Delta \delta \quad \Delta \omega \quad \Delta E'_q \quad \Delta E_{fd} \quad \Delta V_{dc} \quad \Delta V_{se}]^T \quad (23)$$

$$U = [\Delta m_{E,1} \quad \Delta \delta_{E,1} \quad \Delta m_{E,2} \quad \Delta \delta_{E,2}]^T \quad (24)$$

A and B matrices of (22) are considered as follows:

$$A = \begin{bmatrix} 0 & \omega_0 & 0 & 0 & 0 & 0 \\ -\frac{K_1}{M} & 0 & -\frac{K_2}{M} & 0 & -\frac{K_{pd}}{M} & 0 \\ -\frac{K_4}{T'_{d0}} & 0 & -\frac{K_3}{T'_{d0}} & \frac{1}{T'_{d0}} & -\frac{K_{qd}}{T'_{d0}} & 0 \\ -\frac{K_a K_5}{T_a} & 0 & -\frac{K_a K_6}{T_a} & -\frac{1}{T_a} & -\frac{K_a K_{vd}}{T_a} & 0 \\ K_7 & 0 & K_8 & 0 & -K_9 & 0 \\ K_{10} & 0 & K_{11} & 0 & K_{12} & 0 \end{bmatrix} \quad (25)$$

$$B = \begin{bmatrix} 0 & 0 & 0 & 0 \\ -\frac{K_{p,E,1}}{M} & -\frac{K_{p,\delta E,1}}{M} & -\frac{K_{p,E,2}}{M} & -\frac{K_{p,\delta E,2}}{M} \\ -\frac{K_{q,E,1}}{T'_{d0}} & -\frac{K_{q,\delta E,1}}{T'_{d0}} & -\frac{K_{q,E,2}}{T'_{d0}} & -\frac{K_{q,\delta E,2}}{T'_{d0}} \\ -\frac{K_a K_{v,E,1}}{T_a} & -\frac{K_a K_{v,\delta E,1}}{T_a} & -\frac{K_a K_{v,E,2}}{T_a} & -\frac{K_a K_{v,\delta E,2}}{T_a} \\ K_{c,E,1} & K_{c,\delta E,1} & K_{c,E,2} & K_{c,\delta E,2} \\ K_{s,E,1} & K_{s,\delta E,1} & K_{s,E,2} & K_{s,\delta E,2} \end{bmatrix} \quad (26)$$

It is possible to design an appropriate controller using (22) and select the most proper input signal of UPFC from four input signals according to criteria detailed in the next section in order to maintain the system stability and to control the damping of power system against the rotor oscillations of investigated system's synchronous generator. Therefore, it is important to select and design appropriate input signal and desirable damping controller.

UPFC Damping Controller

The linearized model of the UPFC installed in power system explained in (22) can be shown in Fig. 3 [Wang (1997), Shahir (2012)]. The UPFC damping controller consists of two sections of input signal and UPFC controller. The input signal is applied on power system through the input transfer functions of $K_O(s)$, $K_L(s)$, and $K_C(s)$. The state space equation obtained in (22) can be considered as follows [Wang (1997), Shahir (2012)]:

$$\begin{bmatrix} \Delta \delta \\ \Delta \dot{\omega} \\ \dot{z}_m \end{bmatrix} = \begin{bmatrix} 0 & \omega_0 & 0 \\ -k_m & -d_m & -a_{d23} \\ a_{d31} & a_{d32} & a_{d33} \end{bmatrix} \begin{bmatrix} \Delta \delta \\ \Delta \omega \\ z_m \end{bmatrix} + \begin{bmatrix} 0 \\ -b_{d2} \\ -b_{d3} \end{bmatrix} U \quad (27)$$

$$Y = [c_{d1} \quad c_{d2} \quad c_{d3}] \begin{bmatrix} \Delta \delta \\ \Delta \omega \\ z_m \end{bmatrix} + DU \quad (28)$$

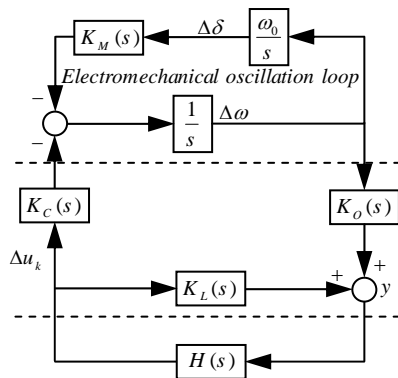


FIG.3 THE CLOSED LOOP BLOCK DIAGRAM MODEL FOR UPFC DAMPING CONTROLLER

In (27), k_m and d_m are the synchronizer and damper

components, respectively, and z_m consists of other state variables of (22). The oscillation angular frequency is obtained by $\omega_i = \sqrt{\omega_0 k_m}$. Here, the transfer functions presented in [Wang (1997), Shahir (2012)] are explained using (27) and (28).

$K_C(s)$ is the transfer function from U input to $\Delta \dot{\omega}$ and obtained as follows:

$$K_C(s) = a_{d23}(sI - a_{d33})^{-1}b_{d3} + b_{d2} \quad (29)$$

$K_O(s)$ is the function of transferring rotor speed to the y measuring point shown in block diagram of Fig. 3 and denoted as follows:

$$K_O(s) = c_{d3}(sI - a_{d33})^{-1} \left(a_{d31} \frac{\omega_0}{s} + a_{d32} \right) + \left(\frac{\omega_0}{s} c_{d1} + c_{d2} \right) \quad (30)$$

$K_L(s)$ is the function of transferring U input to the y measuring point shown in Fig. 3 and calculated as follows:

$$K_L(s) = c_{d3}(sI - a_{d33})^{-1}b_{d3} + D \quad (31)$$

$K_m(s)$ is the transfer function of $\Delta \delta$ to $\Delta \dot{\omega}$ and calculated as follows:

$$K_m(s) = k_m + \frac{s}{\omega_0} d_m + a_{d23}(sI - a_{d33})^{-1} \left(a_{d31} + \frac{s}{\omega_0} a_{d32} \right) \quad (32)$$

$H(s)$, as a UPFC controller transformer, controls the operation of the system shown in Fig. 1 for different input signal values. In this investigation, the UPFC damping controller is considered ideal. An ideal UPFC damping controller should provide a pure positive electric torque in oscillation loop, damp electromechanical oscillations, and stabilize the generator rotor oscillations. Considering Fig. 3, the provided electric torque by UPFC damping controller could be calculated as follows [Wang (1997), Shahir (2012)]:

$$\Delta T_{UPFC} = \frac{K_C(s)K_O(s)H(s)}{1 - K_L(s)H(s)} \Delta \omega \quad (33)$$

The torque magnitude provided by UPFC damping controller is expressed as follows:

$$\Delta T_{UPFC} = D_{UPFC} \Delta \omega \quad (34)$$

D_{UPFC} reduces the generator rotor oscillations. Considering (33) and (34), D_{UPFC} can be regarded as follows:

$$D_{UPFC} = \frac{K_C(s)K_O(s)H(s)}{1 - K_L(s)H(s)} \quad (35)$$

It can be simplified as follows:

$$D_{UPFC} = (K_C(s)K_O(s) + D_{UPFC}K_L(s))H(s) = F(s)H(s) \quad (36)$$

$F(s)$ in (36) varies with power system operation conditions and is defined as follows:

$$F(s) = K_C(s)K_O(s) + D_{UPFC}K_L(s) \quad (37)$$

The operation conditions of the power system, applying UPFC structure presented in [Sadigh (2010)] as a damping controller, depend on the generator operation point, power system condition, and the UPFC input signal. Considering this fact, the selection of UPFC input signals and the most proper of them should be in away that the system stability against electromechanical oscillations is bonded and it achieves its stability as soon as possible. Also, the system should maintain its stability as electromechanical oscillations occur while the damping speed in a power system is highly important. As the damping time is long, the power system would get damaged.

UPFC Damping Controller Design

If it is assumed that a power system has the operation domain of $\Psi(\mu)$, $F(s)$ would be a function of operation condition of μ and UPFC input signal and the controller is designed and installed on power system on this base. The desired controller for oscillation damping is the one that can guarantee the system stability, can acceptably react against the generator rotor oscillations, and can damp such oscillations in the shortest time. Proper input signal selection is one of the most important steps in the design of an appropriate controller. For a good controller designing, several approaches have been evaluated. In this paper, the phase compensation method is applied [Chandrakar (2010)]. For proper control signal selection of UPFC damping controller, three techniques presented in [Wang (1997), Shahir (2012)] are applied in the following subsections.

1) First Technique

The parameter $\Psi(\mu)$ based proper control signal selection for UPFC damping controller design is as follows:

$$\mu_{selected} = \min_{\mu} F(s, \mu, u_k) \quad \mu \in \Psi(\mu) \quad (38)$$

Here, the selection aims to making it possible to design UPFC damping controller in a way that the system would be able to maintain its stability against rotor oscillations under any circumstance. This is accomplished targeting proper control signal selection in order to obtain the power system stability in minimum value of $\Psi(\mu)$.

2) Second Technique

One of the most important issues considered in the designing process of damping controllers is to achieve the maximum control domain with

minimum expense. Therefore, the proper input signal is the one that has the maximum effect on UPFC damping controller. Proper input signal for UPFC damping controller design on the basis of achieving minimum control system costs and maximum control signal effect is shown in (39):

$$u_{selected} = \max_{u_k} F(s, \mu_{selected}, u_k) \quad (39)$$

$$u_k \in m_{E,1}, m_{E,2}, \delta_{E,1}, \delta_{E,2}$$

3) Third Technique

In third technique, (40) is applied to select the most appropriate input signal considering system operation domain, $\Psi(\mu)$. This is done under several conditions of $\Psi(\mu)$ to guarantee the power system condition and tries to select an input signal that would not considerably vary as $\Psi(\mu)$ varies and has a constant and invariable reaction against generator rotor oscillations in $\Psi(\mu)$ domain. If the influence of damping is increased, other system parameters and its operation condition under different $\Psi(\mu)$ values might be undesirably affected. On the other hand, significant decrease in the influence of damping controller can decrease system stability level and make the power system unreliable. In (40), a technique is introduced to achieve power system stability against rotor oscillations with the least impact on other power system parameters and components. However, in the cases, the results are not meaningful or not expectable; it is possible to apply (39) to guarantee the results obtained from (40) for input signal selection of damping controller designing.

$$u_{selected} = \frac{\max_{\mu} F(s, \mu, u_k) - \min_{\mu} F(s, \mu, u_k)}{\min_{\mu} F(s, \mu, u_k)} \quad (40)$$

UPFC Controller Design

As shown in Fig. 3, the UPFC damping controller consists of $H(s)$ feedback transfer function. In [Shahir (2012)], the $H(s)$ function is investigated in conventional UPFCs damping controllers applied in single-machine power systems. In this paper, by developing the method in [Shahir (2012)], $H(s)$ is considered as follows:

$$H(s) = \frac{sT_w}{1+sT_w} \cdot \frac{K_u}{1+sT_u} \cdot \frac{1+sT_2}{1+sT_1} \cdot \frac{1+sT_4}{1+sT_3} \quad (41)$$

Relation (41) can be expressed as follows:

$$H(s) = |H| \angle \theta \quad (42)$$

where $|H|$ is the amplitude and θ is the phase angle

of $H(s)$. Considering (37), $F(s)$ is rewritten as follows:

$$F(s) = |F| \angle \phi \quad (43)$$

In (43), $|F|$ is the amplitude and ϕ is the phase angle of $F(s)$. Both $H(s)$ and $F(s)$ transfer functions considerably affect D_{UPFC} and oscillation damping capability of power system (see (36)).

In UPFC damping controller design, the controller tries to apply a pure positive torque on investigated system using the phase compensation technique. Based on (36), $F(s)$ is a function of $\Psi(\mu)$ and it is possible to achieve an ideal controller that provides positive torque for generator oscillations damping, just by controlling $H(s)$ parameters. Considering (36) and (42), in order to provide a pure positive torque and to design on phase compensation technique, the following relation is valid:

$$H = \frac{D_{UPFC}}{F} \quad \angle \theta = \angle -\phi \quad (44)$$

where the amplitude and the phase angle of $H(s)$ is obtained and regulated by (44).

Simulation Results

One of the most important aims of UPFC installation is to control power system against low frequency oscillations happening as a distortion occurs in power system and the generator rotor is driven out of its synchronous mode. UPFC is in charge of proper responding as such oscillation occurs. Fig. 4 shows the power system illustrated in Fig. 1, where the $\Delta\omega$ error signal is sampled and applied to UPFC through U input signals. In the next parts, the proper signal is selected through analytic methods and UPFC controller regulation approaches are given. Nonlinear simulation is then accomplished on the investigated system.

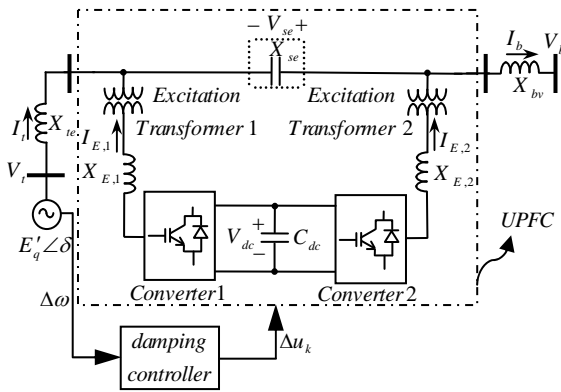


FIG. 4 UPFC TO SIMB CONNECTION

Proper Input Signal Selection

$F(s)$ is a function of UPFC damping controller input signals (37) and directly relates to $\Psi(\mu)$ and varies with $\Psi(\mu)$ and changes ΔT_{UPFC} magnitude. Therefore, $F(s)$ can be applied as a parameter of UPFC controller signals evaluation and the most proper control signal recognition. The most proper UPFC controller signal is selected utilizing techniques introduced in previous section and investigating $F(s)$ under different $\Psi(\mu)$ conditions considered as Table 1 in this paper. The magnitudes and the angles shown in Table 2 are obtained evaluating $F(s)$ under μ_1 and μ_2 operation condition applying Nichols [Wang (1997), Shahr (2012)] approach. Fig. 5 shows the oscillation frequency in $\Psi(\mu)$. It is initially observed that the control system is stable for all $\Psi(\mu)$ values if the control system is designed under μ_2 operation condition. However, this requires further attention especially about the UPFC device applied in this paper whose operation is controlled by four input signals of $\Delta m_{E,1}$, $\Delta m_{E,2}$, $\Delta \delta_{E,1}$, and $\Delta \delta_{E,2}$. In conventional UPFCs applied in power systems, the number of input signals is decreased to three signals and the investigations are carried out on these three inputs due to the incapability of using $\Delta \delta_b$ [Wang (1997)], the phase angle deviation rate of the series voltage-source voltage.

TABLE 1 SYSTEM OPERATION CONDITION IN $\Psi(\mu)$ DOMAIN

operation condition	V_t	V_b	P_e
μ_1	1.0 pu	1.0 pu	0.1 pu
μ_2	1.0 pu	1.0 pu	1.0 pu

TABLE 2 THE AMPLITUDE AND PHASE ANGLE OF $F(s)$ UNDER μ_1 AND μ_2 OPERATING CONDITION

u_k	$ F(s) $ to dB		phase angle to degree	
	μ_1	μ_2	μ_1	μ_2
$m_{E,1}$	32.3789	419.6940°	294.8861°	0.2160
$\delta_{E,1}$	134.9189	430.3020°	407.4034°	12.1071
$m_{E,2}$	14.8118	124.6427°	313.9723°	1.4827
$\delta_{E,2}$	41.7253	507.4505°	300.6187°	0.3162

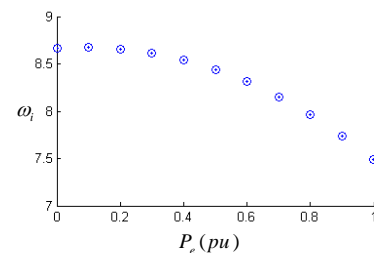


FIG. 5 OSCILLATION FREQUENCY CREATED IN INVESTIGATED SYSTEM

1) Case study 1

In this section, the approach mentioned in (38) is applied to detect the controller signal. Based on (38), the signal that has the minimum value under μ_1 operation condition can be selected. Therefore, applying (38) and based on the results shown in Table 2 results for the most proper signals of controller design are $m_{E,1}$ and $\delta_{E,2}$, respectively.

2) Case study2

Relation (39) selects the controller signal under μ_2 operation condition in a way that the input signal has the maximum amplitude. Therefore, based on the results shown in Table 2, the proper signal for controller design is $\delta_{E,1}$.

3) Case study 3

Considering (40) and Table 2, and selecting $u_k = m_{E,1}$, $u_k = \delta_{E,1}$, $u_k = m_{E,2}$, and $u_k = \delta_{E,2}$, as different input signals, the optimal input signal ($u_{selected}$) is obtained using $u_k = m_{E,1}$.

UPFC Controller Parameters Regulation

As mentioned before, the UPFC controller parameters are regulated applying phase compensation technique (relation (44)). The UPFC controller parameters displace the Eigen values and are regulated in terms of UPFC damping controller input signals in order to create desired D_{UPFC} in $\Psi(\mu)$ for generator rotor oscillations damping and maintain system stability [Shahir (2012)]. As the system Eigen values are less in terms of a specific input signal in damping controller, the input signal is more effective in damping controller and as the UPFC controller gain is less, lower K_U , the UPFC damping controller can be designed and utilized with lower cost. The UPFC controller parameters applied in this paper are as $T_1 = 0.9s$, $T_3 = 0.9s$, $T_u = 0.01s$, and $T_w = 10s$. Other UPFC controller parameters are obtained from (44) by input signal change. The system Eigen values and other UPFC damping controller parameters are respectively shown in Table 3 and Table 4 under μ_1 and μ_2 in terms of different input signals. Based on the results shown in Table 3, the most appropriate signals for UPFC controller input under μ_1 operation condition is $\delta_{E,1}$ from effectiveness point of view and is $m_{E,2}$ from the view point of cost. Based on the

results obtained from system analysis in terms of each UPFC damping controller signals, the maximum damping is achieved selecting $\delta_{E,1}$ as the UPFC damping controller input signal while the minimum cost is achieved under μ_2 operation condition in which $m_{E,2}$ is selecting.

TABLE 3 UPFC CONTROLLER PARAMETER UNDER μ_1

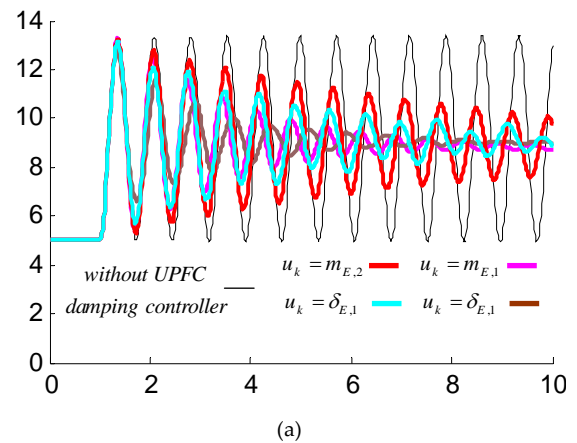
Input signal	UPFC controller parameters	Eigen values
$m_{E,1}$	$K_u = 0.9, T_2 = 0.2, T_4 = 0.15$	$s = -0.1302 \pm j0.0460$
$\delta_{E,1}$	$K_u = 2.3, T_2 = 0.12, T_4 = 0.10$	$s = -0.4718 \pm j0.3120$
$m_{E,2}$	$K_u = 0.6, T_2 = 0.65, T_4 = 0.09$	$s = -0.1368 \pm j0.0101$
$\delta_{E,2}$	$K_u = 0.9, T_2 = 0.55, T_4 = 0.20$	$s = -0.2381 \pm j0.1167$

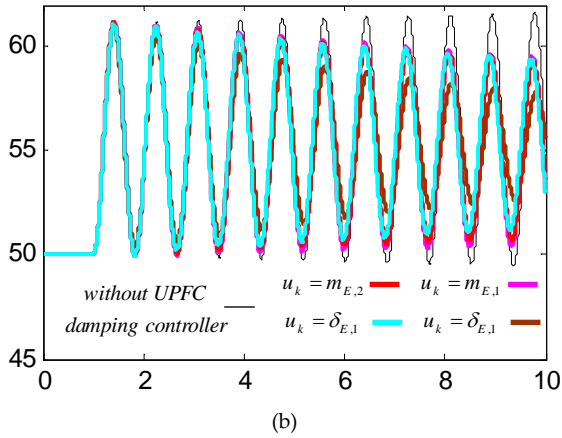
TABLE 4 UPFC CONTROLLER PARAMETER UNDER μ_2

Input signal	UPFC controller parameters	Eigen values
$m_{E,1}$	$K_u = 1.1, T_2 = 0.95, T_4 = 0.95$	$s = -0.0470 \pm j0.0747$
$\delta_{E,1}$	$K_u = 0.65, T_2 = 0.25, T_4 = 0.15$	$s = -0.2074 \pm j0.3264$
$m_{E,2}$	$K_u = 0.3, T_2 = 0.72, T_4 = 0.65$	$s = -0.0727 \pm j0.0241$
$\delta_{E,2}$	$K_u = 3.3, T_2 = 0.65, T_4 = 0.45$	$s = -0.0903 \pm j0.0003$

Nonlinear Analysis

In this section, the system shown in Fig. 1 is simulated under relations mentioned in (1)-(6). The aim is to investigate the way system responds to sudden load variation caused by distortions. The simulation is carried out under the circumstance that a three-phase to ground fault occurs in the system shown in Fig. 1. The fault occurs in $t = 1$ sec. In this simulation, the operation condition of the system is as Table 1. Other simulation parameters are detailed in Appendix C. Fig. 6(a) shows the simulation results under μ_1 operation condition. The results are evaluated for all four input signals. The system condition during distortion occurrence without applying UPFC damping controller is shown in Fig. 6(a).



FIG. 6 SIMULATION RESULTS (a) UNDER μ_1 (b) UNDER μ_2

Under such condition, the system starts to oscillate and the stability is weakened. Also, Fig. 6(a) shows the system condition under distortion occurrence and at the presence of UPFC damping controller designed for $m_{E,1}$, $\delta_{E,1}$, $m_{E,2}$ and $\delta_{E,2}$ input signals, respectively. According to the results shown in the figure, the system stability is reinforced and the oscillations are rapidly damped under μ_1 and applying $u_k = \delta_{E,1}$, while the system damping is slow under $u_k = m_{E,2}$ condition, which leads to the defection of the power system equipments. Fig. 6(b) shows the system response to the created distortion when it operates under μ_2 operation condition. In this figure, it is illustrated that the investigated system oscillates if no UPFC damping controller is applied. Also, Fig. 6(b), shows the assessment results of system damping rate improve the application of UPFC input signals and the damping controller for $m_{E,1}$, $\delta_{E,1}$, $m_{E,2}$ and $\delta_{E,2}$, respectively. According to the results shown in Fig. 6(b), the system is more stable against the oscillations with $u_k = \delta_{E,1}$. Also, it is not reliable with $u_k = \delta_{E,2}$ and the oscillations are damped very slowly.

Conclusions

Although several approaches are used to select proper input signals, different standards can be considered to select such signals for UPFC damping controller installed in power systems (such as the system investigated in this paper). If the purpose of damping controller design is just to control generator rotor oscillations and the economical concerns are not under consideration, the most appropriate UPFC damping controller signal is the one applied to system desirably in all $\Psi(\mu)$ and damps oscillations rapidly and controls the system. Therefore, it is possible to utilize $m_{E,2}$ as input signal. If the economical concerns and

costs reduction interests are considered in power systems designing process, the proper controller is the one that possesses lower UPFC controller gain for specific input signal in all $\Psi(\mu)$ domains. Therefore, $\delta_{E,1}$ can be the most appropriate option. The stability of the controllers designed in power system is significantly important. The stability of the designed controller can be explained as such statement that the damping controller input signal is effective in all $\Psi(\mu)$ domains and operates invariably. Considering such a standard, selecting $m_{E,1}$ can guarantee the designed controller's stability in all $\Psi(\mu)$ domains.

APPENDIX A

The constants used in (1)-(6) is as follows:

$$\begin{aligned}
 a_1 &= \left[\frac{X_{a3}(X_{te} - X_{E,1})}{X_1 X_{E,1}} \right]; \quad a_2 = \left(\frac{-X_{a3} X_{te}}{X_1 X_{E,1}} \right); \\
 a_3 &= \frac{1}{jX_{BB}} (1 - jX_2 X_{a3}); \quad b_1 = \left[\frac{(X_{E,1} - X_{te})(X_{a3} + X_{a2})}{X_1 X_{E,1}} \right]; \\
 b_2 &= \left[\frac{X_{te}(X_{a3} - X_{a2})}{X_1 X_{E,1}} \right]; \quad b_3 = \frac{1}{X_{BB}} \left[X_2 (X_{a3} + X_{b2}) + \left(\frac{X_{E,2}}{X_{E,1}} \right) \right]; \\
 c_1 &= \left[\frac{(X_{a2} + X_{b3} + X_{b2})(X_{E,1} - X_{te}) + jX_1}{X_1 X_{E,1}} \right]; \\
 c_2 &= \left[\frac{X_{te}(X_{a2} + X_{b3} + X_{b2}) - jX_1}{X_1 X_{E,1}} \right]; \\
 c_3 &= \frac{1}{jX_{BB} \left[-\frac{X_{bv}}{X_{E,1}} + jX_2 (X_{a3} + X_{b3} + X_{a2}) \right]}; \\
 d_1 &= \left[\frac{(X_{te} - X_{E,1})(X_{b3} + X_{b2}) - jX_1}{X_1 X_{E,1}} \right]; \\
 d_2 &= \left[\frac{-X_{te}(X_{b3} + X_{b2}) + jX_1}{X_1 X_{E,1}} \right]; \\
 d_3 &= \frac{1}{jX_{BB} \left[-jX_2 (X_{b3} + X_{b2}) + \left(\frac{X_{bv}}{X_{E,1}} \right) \right]}
 \end{aligned}$$

APPENDIX B

The constants used in (11)-(15) are as follows:

$$\begin{aligned}
 K_1 &= [(a_1 + a_2)(V_{t,q} + X_q I_{t,d})]V_b \cos \delta \\
 &\quad - [(a_1 + a_2)(V_{t,d} - X'_d I_{t,q})]V_b \sin \delta \\
 K_2 &= (V_{t,d} - X'_d I_{t,q})(c_1 + c_2), \quad K_6 = (c_1 + c_2) + \left(\frac{V_{t,d}}{V_t} \right) \\
 K_3 &= 1 + (X_d - X'_d)(c_1 + c_2), \quad K_4 = -(a_1 + a_2)V_b \sin \delta \\
 K_5 &= (a_1 + a_2)X'_d V_b \sin \delta + (a_1 + a_2) \left(\frac{V_{t,d}}{V_t} \right) X_q V_b \cos \delta
 \end{aligned}$$

$$\begin{aligned}
K_7 &= \frac{3a_3 m_{E,2} V_b}{4C_{dc}} (\cos \delta \sin \delta_{E,2} - \sin \delta \cos \delta_{E,2}) \\
&\quad + \frac{3a_2 m_{E,1} V_b}{4C_{dc}} (\cos \delta \sin \delta_{E,1} - \sin \delta \cos \delta_{E,1}) \\
K_8 &= \frac{3c_3 m_{E,2}}{4C_{dc}} (\cos \delta_{E,2}) + \frac{3c_2 m_{E,1}}{4C_{dc}} (\cos \delta_{E,1}) \\
K_9 &= -\frac{3m_{E,2}}{4C_{dc}} (f_1 \cos \delta_{E,2} + f_2 \sin \delta_{E,2}) \\
&\quad - \frac{3m_{E,1}}{4C_{dc}} (f_3 \cos \delta_{E,1} + f_4 \sin \delta_{E,1}) \\
K_{10} &= -\frac{a_1 V_b}{C_{se}} (\sin \delta + \cos \delta), \quad K_{11} = \frac{c_1}{C_{se}} \\
K_{12} &= \frac{b_1 m_{E,2}}{2C_{se}} (\cos \delta_{E,2} + \sin \delta_{E,2}) + \frac{d_1 m_{E,1}}{2C_{se}} (\cos \delta_{E,1} + \sin \delta_{E,1}) \\
K_{s,E,1} &= \frac{d_1 V_{dc}}{2C_{se}} (\cos \delta_{E,1} + \sin \delta_{E,1}), \\
K_{s,E,2} &= \frac{b_1 V_{dc}}{2C_{se}} (\cos \delta_{E,2} + \sin \delta_{E,2}) \\
K_{s,\delta E,1} &= \frac{d_1 m_{E,1} V_{dc}}{2C_{se}} (\cos \delta_{E,1} - \sin \delta_{E,1}) \\
K_{s,\delta E,2} &= \frac{b_1 m_{E,2} V_{dc}}{2C_{se}} (\cos \delta_{E,2} - \sin \delta_{E,2}) \\
K_{qd} &= \left(\frac{b_1 + b_2}{2} \right) m_{E,2} \cos \delta_{E,2} + \left(\frac{d_1 + d_2}{2} \right) m_{E,1} \cos \delta_{E,1} \\
K_{pd} &= (V_{t,d} - X'_d I_{t,q}) \left[\left(\frac{b_1 + b_2}{2} \right) m_{E,2} \cos \delta_{E,2} + \right. \\
&\quad \left. \left(\frac{d_1 + d_2}{2} \right) m_{E,1} \cos \delta_{E,1} \right] + (V_{t,q} + X_q I_{t,d}) \\
&\quad \left[\left(\frac{b_1 + b_2}{2} \right) m_{E,2} \sin \delta_{E,2} + \left(\frac{d_1 + d_2}{2} \right) m_{E,1} \sin \delta_{E,1} \right] \\
K_{vd} &= \left(\frac{V_{t,d}}{V_t} \right) \left[\left(\frac{b_1 + b_2}{2} \right) m_{E,2} \sin \delta_{E,2} + \left(\frac{d_1 + d_2}{2} \right) m_{E,1} \sin \delta_{E,1} \right] \\
&\quad X_q - \left[\left(\frac{b_1 + b_2}{2} \right) m_{E,2} \cos \delta_{E,2} + \left(\frac{d_1 + d_2}{2} \right) m_{E,1} \cos \delta_{E,1} \right] X'_d \\
K_{q,E,1} &= \left(\frac{d_1 + d_2}{2} \right) V_{dc} \cos \delta_{E,1}, \\
K_{q,E,2} &= \left(\frac{b_1 + b_2}{2} \right) V_{dc} \cos \delta_{E,2} \\
K_{q,\delta E,1} &= -\left(\frac{d_1 + d_2}{2} \right) m_{E,1} V_{dc} \sin \delta_{E,1} \\
K_{q,\delta E,2} &= -\left(\frac{b_1 + b_2}{2} \right) m_{E,2} V_{dc} \sin \delta_{E,2} \\
K_{p,E,1} &= \left(\frac{d_1 + d_2}{2} \right) [(V_{t,d} - X'_d I_{t,q}) \cos \delta_{E,1} \\
&\quad + (V_{t,q} + X_q I_{t,d}) \sin \delta_{E,1}] V_{dc}
\end{aligned}$$

$$\begin{aligned}
K_{p,E,2} &= (V_{t,q} + X_q I_{t,d}) \left(\frac{b_1 + b_2}{2} \right) V_{dc} \sin \delta_{E,2} \\
&\quad - (a_1 + a_2) (V_{t,d} - X'_d I_{t,q}) V_b \sin \delta \\
K_{p,\delta E,1} &= \left(\frac{d_1 + d_2}{2} \right) [(V_{t,q} + X_q I_{t,d}) \cos \delta_{E,1} \\
&\quad - (V_{t,d} - X'_d I_{t,q}) \sin \delta_{E,1}] m_{E,1} V_{dc} \\
K_{p,\delta E,2} &= \left[(V_{t,q} + X_q I_{t,d}) \left(\frac{b_1 + b_2}{2} \right) \right] m_{E,2} V_{dc} \cos \delta_{E,2} \\
&\quad - \left(\frac{b_1 + b_2}{2} \right) (V_{t,d} - X'_d I_{t,q}) m_{E,2} V_{dc} \sin \delta_{E,2} \\
K_{c,E,1} &= \frac{3d_3 m_{E,2} V_{dc}}{8C_{dc}} (\cos \delta_{E,1} \cos \delta_{E,2} + \sin \delta_{E,1} \sin \delta_{E,2}) \\
&\quad + \frac{3d_2 m_{E,1} V_{dc}}{8C_{dc}} (\cos \delta_{E,1}^2 + \sin \delta_{E,1}^2) + w_1 \\
K_{c,E,2} &= \frac{3b_3 m_{E,2} V_{dc}}{8C_{dc}} (\cos \delta_{E,2}^2 + \sin \delta_{E,2}^2) \\
&\quad + \frac{3b_2 m_{E,1} V_{dc}}{8C_{dc}} (\cos \delta_{E,2} \cos \delta_{E,1} + \sin \delta_{E,2} \sin \delta_{E,1}) + w_2 \\
K_{c,\delta E,1} &= \frac{3d_3 m_{E,2} m_{E,1} V_{dc}}{8C_{dc}} (-\sin \delta_{E,1} \cos \delta_{E,2} + \cos \delta_{E,1} \sin \delta_{E,2}) \\
&\quad + \frac{3d_2 m_{E,1}^2 V_{dc}}{8C_{dc}} (-\sin \delta_{E,1} \cos \delta_{E,1} + \cos \delta_{E,1} \sin \delta_{E,1}) + w_3 \\
K_{c,\delta E,2} &= \frac{3b_3 m_{E,2}^2 V_{dc}}{8C_{dc}} (-\sin \delta_{E,2} \cos \delta_{E,2} + \cos \delta_{E,2} \sin \delta_{E,2}) \\
&\quad + \frac{3b_2 m_{E,1} m_{E,2} V_{dc}}{8C_{dc}} (-\sin \delta_{E,2} \cos \delta_{E,1} + \cos \delta_{E,2} \sin \delta_{E,1}) + w_4 \\
K_{v,E,1} &= \left(\frac{d_1 + d_2}{2} \right) \left[\left(\frac{V_{t,d}}{V_t} \right) X_q \sin \delta_{E,1} - \left(\frac{d_1 + d_2}{2} \right) \right. \\
&\quad \left. X'_d \cos \delta_{E,1} \right] V_{dc} \\
K_{v,E,2} &= \left(\frac{V_{t,d}}{V_t} \right) \left(\frac{b_1 + b_2}{2} \right) X_q V_{dc} \sin \delta_{E,2} - \left(\frac{b_1 + b_2}{2} \right) X'_d V_{dc} \cos \delta_{E,2} \\
K_{v,\delta E,1} &= \left(\frac{d_1 + d_2}{2} \right) X'_d m_{E,1} V_{dc} \sin \delta_{E,1} + \left(\frac{V_{t,d}}{V_t} \right) X_q m_6 \\
K_{v,\delta E,2} &= \left(\frac{V_{t,d}}{V_t} \right) \left(\frac{b_1 + b_2}{2} \right) X_q m_{E,2} V_{dc} \cos \delta_{E,2} \\
&\quad + \left(\frac{b_1 + b_2}{2} \right) X'_d m_{E,2} V_{dc} \sin \delta_{E,2} \\
f_1 &= \left(\frac{b_3}{2} \right) m_{E,2} \cos \delta_{E,2} + \left(\frac{d_3}{2} \right) m_{E,1} \cos \delta_{E,1} \\
f_2 &= \left(\frac{b_3}{2} \right) m_{E,2} \sin \delta_{E,2} + \left(\frac{d_3}{2} \right) m_{E,1} \sin \delta_{E,1} \\
f_3 &= \left(\frac{b_2}{2} \right) m_{E,2} \cos \delta_{E,2} + \left(\frac{d_2}{2} \right) m_{E,1} \cos \delta_{E,1}
\end{aligned}$$

$$\begin{aligned}
f_4 &= \left(\frac{b_2}{2}\right) m_{E,2} \sin \delta_{E,2} + \left(\frac{d_2}{2}\right) m_{E,1} \sin \delta_{E,1} \\
w_1 &= \left(\frac{3}{4C_{dc}}\right) I_{E,1,d} \cos \delta_{E,1} + \frac{3}{4C_{dc}} I_{E,1,q} \sin \delta_{E,1} \\
w_2 &= \left(\frac{3}{4C_{dc}}\right) I_{E,2,d} \cos \delta_{E,2} + \left(\frac{3}{4C_{dc}}\right) I_{E,2,q} \sin \delta_{E,2} \\
w_3 &= \left(\frac{3m_{E,1}}{4C_{dc}}\right) I_{E,1,q} \cos \delta_{E,1} - \left(\frac{3m_{E,1}}{4C_{dc}}\right) I_{E,1,d} \sin \delta_{E,1} \\
w_4 &= \left(\frac{3m_{E,2}}{4C_{dc}}\right) I_{E,2,q} \cos \delta_{E,2} - \left(\frac{3m_{E,2}}{4C_{dc}}\right) I_{E,2,d} \sin \delta_{E,2}
\end{aligned}$$

APPENDIX C

The investigated power system parameters used in simulation process are as follows:

$$\begin{aligned}
\delta_{E,1} &= 30^\circ; \delta_{E,2} = -25^\circ; X_{E,1} = X_{E,2} = 0.2 pu; \\
X_{se} &= X_{te} = 0.1 pu; X_{bv} = X_d = 1.0 pu; X_q = 0.6 pu; \\
X_d' &= 0.3 pu; C_{dc} = C_{se} = 3.0 pu; m_{E,1} = m_{E,2} = 1; \\
V_{dc} &= E_q' = 2.0 pu; V_b = 1.0 pu; M = 2H = 8.0 s; \\
f_s &= 50 Hz; T_{do}' = 5.044 s; T_a = 0.05 s; K_a = 50; D_m = 0
\end{aligned}$$

REFERENCES

- Chandrakar V.K., Dhurvey S.N., and Suke S.C., "Performance comparison of SVC with POD and PSS for damping of power system oscillations," in Proc. ICETET, 2010, pp. 247-252.
- Fang W. and Ngan H. W., "Enhancing small signal power system stability by coordinating unified power flow controller with power system stabilizer," *Electr. Power Syst. Res.*, Vol. 65, No. 2, 2003, pp. 91-99.
- Higorani N.G. and Gyugyi L., "Understanding FACTS: concepts and technology of flexible ac transmission systems," IEEE Press, New Jersey, 1999.
- Kundur P., "Power system stability and control," McGraw-Hill Press, New York, 1994.
- Larsen E.V., Sanchez-Gasca J.J., and Chow J.H., "Concept for design of FACTS controllers to damp power swings," *IEEE Trans. Power Syst.*, Vol. 10, No. 2, 1995, pp. 948-956.
- Sadigh A.K., Hagh M.T., and Sabahi M., "Unified power flow controller based on two shunt converters and a series capacitor," *Electr. Power Syst. Res.*, Vol. 80, No. 12, 2010, pp. 1511-1519.
- Saravana Ilango G., Nagamani C., Sai A.V.S.S.R., and Aravindan D., "Control algorithms for control of real and reactive power flows and power oscillation damping using UPFC," *Electr. Power Syst. Res.*, Vol. 79, No. 4, 2009, pp. 595-605.
- Shahir F.M., Babaei E., Ranjbar S., and Torabzad S., "New Control Methods for Matrix Converter based UPFC under Unbalanced Load," in Proc. IICPE, 2012.
- Shahir F.M. and Babaei E., "Evaluation of Power System Stability by UPFC via Two Shunt Voltage-Source Converters and a Series Capacitor," in Proc. of IEEE ICEE, 2012., pp. 318-323.
- Shahir F.M., Babaei E., Ranjbar S., and Torabzad S., "Dynamic Modeling of UPFC based on Indirect Matrix Converter," in Proc. IICPE, 2012.
- Shahir F.M. and Babaei E., "Dynamic Modeling of UPFC by Two Shunt Voltage-Source Converters and a Series Capacitor," in Proc. ICECT, 2012, pp. 554-558.
- Shahir F.M. and Babaei E., "Evaluating the Dynamic Stability of Power System Using UPFC based on Indirect Matrix Converter," in Proc. ICECT, 2012, pp. 548-553.
- Shahir F.M. and Babaei E., "Evaluating the Dynamic Stability of Power System Using UPFC based on Indirect Matrix Converter," *Journals of the Engineering and Technology*, 2013.
- Shahir F.M. and Babaei E., "Dynamic Modeling of UPFC by Two Shunt Voltage-Source Converters and a Series Capacitor," *International Journal of Computer and Electrical Engineering*, 2013.
- Song S.H., Lim J., and Moon S.II., "Installation and operation of FACTS devices for enhancing steady-state security," *Electr. Power Syst. Res.*, Vol. 70, No. 1, 2004, pp. 7-15.
- Sreenivasachar K., Jayaram S., and Salama M.M.A., "Dynamic stability improvement of multi-machine power system with UPFC," *Electr. Power Syst. Res.*, Vol. 55, No. 1, 2000, pp. 27-37.
- Wang H.F. and Swift F.J., "FACTS-based stabilizer designed by the phase compensation method. I. Single-machine infinite-bus power systems. II. Multi-machine power systems," in Proc. APSCOM, 1997, pp. 638-649.
- Xia Jiang Chow J.H., Edris A-A., Fardanesh B., and Uzunovic E., "Transfer path stability enhancement by voltage-sourced converter-based FACTS controller," *IEEE Trans. Power Del.*, Vol. 25, No. 2, 2010, pp. 1019-1025.

Yassami H., Darabi A., and Rafiei S.M.R., "Power system stabilizer design using Strength Pareto multi-objective optimization approach," *Electr. Power Syst. Res.* Vol. 80, No. 7, 2010, pp. 838-846.

Farzad mohammadzadeh Shahir was born in Tabriz, Iran, in 1985. He received the B.S. degree in electronic engineering from Islamic Azad University, Mianeh, Iran, the M.S. degree in electrical engineering from Islamic Azad University, Ahar, Iran, in 2008 and 2011, respectively. In 2004, he joined the Iran Tractor Manufacturing Company, Tabriz, Iran, where he has been an electrical engineering. His current research interests include power system dynamic and power electronic converters.

Ebrahim Babaei was born in Ahar, Iran in 1970. He received his B.S. and M.S. in Electrical Engineering from the Department of Engineering, University of Tabriz, Tabriz, Iran, in 1992 and 2001, respectively, graduated with first class honors. He received his Ph.D. in Electrical Engineering from the Department of Electrical and Computer Engineering, University of Tabriz, Tabriz, Iran, in 2007. In 2004, he joined the Faculty of Electrical and Computer Engineering, University of Tabriz. He was an Assistant Professor from 2007 to 2011 and has been an Associate Professor since 2011. He is the author of more than 210 journal and conference papers. His current research interests include the analysis and control of power electronic converters, matrix converters, multilevel converters, FACTS devices, power system transients, and power system dynamics.